Journal of Applied Polymer Science

Simultaneous measurement of the molecular weight distribution and 5-ethylidene-2-norbornene content across the molecular weight distribution of ethylene–propylene–diene terpolymer via a new size exclusion chromatography–ultraviolet–refractive index method

Z. Zhou,[1] M. Janco,[2] R. Cong,[1] D. Lee,[3] C. Li Pi Shan,[1] P. Boopalachandran,[1] Z. Shi,[1] M. D. Miller,[1] B. Winniford,[1] T. Huang,[1] E. Herceg,[4] I. Salazar,[1] T. Pangburn,[3] A. Sandlin,[1] L. Fan,[1] J. Wu[2]

[1]Dow Chemical Company, Freeport Texas 77541
[2]Dow Chemical Company, Collegeville Pennsylvania 19426
[3]Dow Chemical Company, Midland Michigan 48667
[4]Dow Chemical Company, Union Kentucky 41091
Correspondence to: Z. Zhou (E-mail: zzhou@dow.com)

ABSTRACT: A size exclusion chromatography (SEC)–UV–refractive index (RI) method was developed to measure the 5-ethylidene-2-norbornene (ENB) content across the molecular weight distribution (MWD) in ethylene–propylene–diene terpolymer (EPDM) at room temperature. The ratio of the UV and RI signals at the same effective elution volume was converted to ENB content. The feasibility of using this method to measure the ENB content across the MWD in EPDM at high temperature was also demonstrated. Prior understanding was that ENB had insufficient UV absorbance relative to high-temperature SEC solvents to allow for useful measurements. We demonstrated this by using high-boiling-point solvents, such as decalin, with a low UV absorbance in the UV wavelength range of interest for ENB. These solvents also gave rise to a high enough specific RI increment (dn/dc) for EPDM that a suitable RI detector response was obtained. Additionally, this methodology could be readily applied to other polymers soluble at high temperature as long as the polymers contained a UV chromophore. These include polymers containing vinyl, conjugated vinyl, aromatic ring, carbonyl, or halocarbon groups. This UV-absorption-based detection concept might also be extended to high-temperature thermal-gradient interactive chromatography-UV, high-temperature solvent-gradient interactive chromatography-UV (high-temperature liquid chromatography-UV), temperature-rising elution fractionation-UV, crystallization analysis fractionation-UV, and crystallization elution fractionation-UV. © 2016 Wiley Periodicals, Inc. J. Appl. Polym. Sci. **2016**, *133*, 43911.

KEYWORDS: copolymers; elastomers; polyolefins; properties and characterization; separation techniques

Received 12 April 2016; accepted 12 May 2016
DOI: 10.1002/app.43911

INTRODUCTION

Ethylene–propylene–diene terpolymers (EPDMs) are commercially important hydrocarbon elastomers. They have outstanding resistance properties against ozone, oxidation, aging, weather, and high temperatures.[1–3] EPDMs are used in many applications, for example, automotive weather stripping, hoses, belts, roofing, footwear soling, and general rubbers. 5-Ethylidene-2-norbornene (ENB) is the most widely used diene in EPDM because it leads to faster curing and higher productivity. Its current market share is greater than 90%. The properties of EPDMs are affected by their molecular weight distribution (MWD), comonomer content distribution, and the way these distributions are related to each other, such as how the ENB content varies with the molecular weight.[3]

Size exclusion chromatography (SEC) determines the MWD and the various molecular weight averages of polymers.[4] The molecular weight dependence of the comonomer content can shine a light on the polymerization mechanism and provide a better understanding of the structure–property relationships.[5] It is time-consuming and sometimes it is even unpractical to do fractionation followed by spectroscopic analyses. On-flow SEC–^{1}H NMR is a good method for determining the molecular weight dependence of the comonomer content,[6] tacticity,[7] and end groups[8] of some

Additional Supporting Information may be found in the online version of this article

polymer samples. The ENB distribution with respect to the molecular weight of EPDM was shown with one EPDM, which was soluble in chloroform ($CHCl_3$) at room temperature, by stop-flow SEC–^{1}H NMR, however, because of sensitivity issues, only a few fractions were studied.[5] SEC–UV–refractive index (RI) analysis was applied to an EPDM sample at room temperature with tetrahydrofuran as the eluent to measure the overall unsaturation level, but no ENB distribution information with respect to the molecular weight was obtained.[9]

A high-temperature SEC system was developed to measure the molecular weights and MWDs of low-solubility, superengineering polymers [e.g., poly(phenylene sulfide), poly(ether ether ketone), poly(ethylene terephthalate)] and low-solubility polymers (e.g., polyethylene, polypropylene). 1-Chloronaphthalene was used as a mobile phase at 210 °C. A UV detector/viscometer for poly(phenylene sulfide) and a flame ionization detector/viscometer for polyethylene and polypropylene were used as detectors. The column efficiency at a superhigh temperature was also studied.[10] 1-Cyclohexyl-2-pyrrolidinone was compared with 1-chloronaphthalene as a solvent for SEC of poly(phenylene sulfide). 1-Cyclohexyl-2-pyrrolidinone had a weaker UV absorbance at less than 350 nm compared to 1-chloronaphthalene and thus could be used to measure the MWD of poly(phenylene sulfide) with a UV detector. However, the degradation of poly(phenylene sulfide) occurred during sample preparation, and ionic interaction between poly(phenylene sulfide) and the column packing occurred. These disadvantages were reduced by the use of 1-chloronaphthalene in the sample preparation and by the addition of LiCl to poly(phenylene sulfide). In this system, polystyrene standards could be detected by UV spectroscopy at 275 nm, and the MWD of poly(phenylene sulfide) was measured.[11] Anderson[12] developed a two-step methodology: derivatization with 2,4-dinitrobenzensulfonyl chloride to add a UV-sensitive functional group to the olefinic bonds and allow quantification of the olefinic bond distribution by the ratio of the UV and RI detector signals. This method requires the knowledge of the averaged double-bond content (usually determined by an independent technique) and works with the assumption of quantitative derivatization of the polymer chains, regardless of the molecular weight.

High-temperature SEC can also be coupled with IR to provide ethylene and propylene incorporation along the MWD.[13] However, this method is not sensitive enough to provide ENB distribution information. As most commercial EPDM products are not soluble in organic solvents at room temperature, room-temperature stop-flow SEC–^{1}H NMR cannot be used. No commercial high-temperature SEC–NMR instrument is available, although an article about it was published.[14] The room-temperature SEC–UV–RI discussed previously is also not applicable.[9]

A high-temperature UV detector was developed in the 1980s through the separation of a heated cell from the optical and electrical components of the UV detector.[15] Here we demonstrate the feasibility of an SEC–UV–RI method that allowed the measurement of the ENB content across the MWD in EPDM at high temperature. This was shown by the use of high-boiling-point solvents such as decalin, which were found to have a low UV absorbance in the UV wavelength range of analytical interest for ENB. These solvents also yielded a high enough dn/dc for EPDM that a suitable RI detector response could be obtained. The ratio of the UV and RI signals at the same effective elution volume provided the ENB content. In contrast, prior understanding was that ENB had insufficient UV absorbance relative to high-temperature SEC solvents to make useful measurements. The methodology reported here could also be readily applied to other polymers soluble at high temperature as long as the polymers contain a UV chromophore. This includes polymers containing vinyl, conjugated vinyl, aromatic, carbonyl, or halocarbon groups. This UV-absorption-based detection concept could also be extended to high-temperature thermal-gradient interactive chromatography-UV,[16] high-temperature solvent-gradient interactive chromatography-UV (high-temperature liquid chromatography-UV),[17,18] temperature-rising elution fractionation-UV,[19] crystallization analysis fractionation-UV,[20] crystallization elution fractionation-UV,[21] and other high-temperature hyphenated techniques-UV.

EXPERIMENTAL

Chemicals

The following were used: deuterated chloroform ($CDCl_3$; purity D = 99.8%; Cambridge Isotope Laboratories, Inc.), 1,1,2,2-tetrachloroethane-d_2 (TCE-d_2; purity D = 99.5%; Cambridge Isotope Laboratories), 1,1,2,2-tetrachloroethane (TCE; purity ≥ 97.0%; Sigma-Aldrich), TCE {purity (purum) ≥ 98% [gas chromatography (GC)]; Fluka}, decahydronaphthalene [mixture of cis and trans (decalin); purity (anhydrous) ≥ 99%; Sigma-Aldrich], benzene (thiophene-free; purity = 99 mol %; Fisher Chemical), bromobenzene [purity ≥ 99.5% (GC); Aldrich], methanol [purity = 99.9% (Optima liquid chromatography/mass spectrometry); Fisher Chemical], ethylidenecyclohexane (purity = 99.8%; Aldrich), acetone [purity = 99.7% (Optima); Fisher Chemical], anhydrous dodecane (purity > 99%; Aldrich), and decane (purity > 99%; Acros). Polymers EPDM A and EPDM B were prepared with Insite Technology by Dow Chemical Co. Their compositions were obtained with ^{13}C-NMR, and the results are listed in Table I. Detailed NMR data and the methods used for the calculations are listed in the Supporting Information.

Gas-Phase UV Simulation

All UV computational results were obtained with the Gaussian 09 program package.[22] The optimization of geometries was performed with density functional theory with the three-parameter hybrid Becke exchange and Lee–Yang–Parr correlation method.[23] For carbon and hydrogen atoms, the double-ξ basis function 6-31G* was used consisting of a polarization d function on carbon atoms. Optimized molecular structures were then used in the calculation of the UV spectra. The allowed electronic transitions and excited state energies were calculated with the Zerner-modified semi-empirical intermediate neglect of the differential overlap method[24]; these were incorporated into the Gaussian software. The spectra were simulated by the assumption of the mixed Gaussian (90%) and Lorentzian (10%) line shapes centered at the calculated excitation energies.

UV Measurements

The UV measurements were done on a Shimadzu UV-3600 series spectrometer. The absorbance wavelength of the samples fell in the region between 220 and 300 nm. The UV experimental parameters used to acquire the data are listed in Table II.

Table I. Chemical Compositions of EPDM A and EPDM B (E: ethylene; P: propylene)

Sample	ENB (wt %)	E (wt %)	P (wt %)
EPDM A	5.2	50.4	44.4
EPDM B	1.1	46.1	52.8

GC–UV Analysis

The GC–vacuum ultraviolet (VUV) analysis of ethylidenecyclohexane was performed with an Agilent 7890A GC instrument connected to a VUV GC detector (VGA-100).[25] Ethylidenecyclohexane was eluted around 3 min under the instrumental conditions listed in Table III. Dark and reference scans were collected at the beginning of each chromatographic analysis.

SEC–UV–RI Measurement

Three samples of EPDM polymer, EPDM A, EPDM B, and their 1:1 w/w blend, were prepared in $CHCl_3$ at a concentration of about 10 mg/g and shaken on a mechanical shaker at ambient temperature overnight to bring the polymer into solution. Polymer solutions were filtered with 0.45 μm polytetrafluoroethylene filters into autosampler vials. Some resistance was observed during filtration.

SEC separations were carried out on a liquid chromatograph consisting of an Agilent model 1100 isocratic pump and injector (Waldbronn, Germany), an Eppendorf CH-430 column oven (Madison, WI), and Waters 486 and 410 UV and RI detectors (Milford, MA) connected in series. The UV detector wavelength was set at 250 nm. System control, data acquisition, and data processing were performed with Cirrus software (version 3.1, Polymer Laboratories, part of Agilent, Church Stretton, United Kingdom). SEC separations were performed in $CHCl_3$ (certified grade; Fisher) at 1 mL/min with two PLgel columns (300 × 7.5-mm inner diameter) packed with a polystyrene–divinylbenzene gel (mixed C pore size and 5-μm particle size; Polymer Laboratories, part of Agilent, Church Stretton, United Kingdom). A volume of 100 μL of sample was injected for the SEC separation. The following components were used for the SEC separations with decalin as the solvent: Waters 2695 pump, Shimadzu SIL-20AC autosampler, three PL-Olexis (7.5 × 300 mm) columns, Shimadzu SPD-20A UV detector, and Shodex RI-101 RI detector. The flow rate was 1.0 mL/min. The other conditions are given in the figure captions.

Table II. UV Experimental Parameters

UV–visible experimental parameter	Parameter value/ description
Spectral range	220–900 nm
Integration time	10 s
Blank	DI water
Interval	1 nm
Path length	1 cm (quartz cuvette)

Table III. GC–UV Experimental Conditions

GC	Agilent 7890A
Column	Agilent HP-5MS, 30 m × 0.25 mm, 0.25 μm film
Oven	60 °C, held for 2 min, ramped at 8 °C/min to 290 °C, held for 5 min (total run time = 35.75 min)
Carrier/flow	Hydrogen, 0.8 mL/min, constant flow
Inlet (split/splitless)	250 °C, 200:1 split ratio
Injection volume	0.2 μL
Wash solvent	Methanol
VUV detector	VUV Analytics VGA-100
Transfer line temperature	275 °C
Flow cell temperature	275 °C
Makeup gas pressure	5.0 psi
Dark scan parameters	11 ms scan time, 100 averages
Reference scan parameters	11 ms scan time, 100 averages
Absorption scan parameters	11 ms scan time, 20 averages
Wavelength range scanned	125–240 nm

RESULTS AND DISCUSSION

Gas-Phase Theoretical UV Simulation of the Model Compounds

Our goal was to find a fast, easy to use, inexpensive, and safe method to measure ENB incorporation as a function of the molecular weight. One of the more sensitive measurement techniques is UV absorption spectroscopy. The ENB monomer has a double bond but not a conjugated double bond. Before this study, it was unknown whether the ENB double bond would have sufficient absorbance in the 200–300 nm range to allow quantification in common SEC solvents. It is well known that ethylene has a UV absorbance around 170 nm, but most common SEC solvents also have significant absorbance in this region. However, three protons on the double bond in ENB are substituted by carbons. To understand the substitution effect on the UV absorbance, the gas-phase theoretical UV simulation of ethylene, propene, 2-methyl-2-propene, *cis*-2-butene, and 2-methyl-2-butene were conducted (Figure 1). There were two absorbance peaks for each chemical; these corresponded to σ–σ^* and π–π^* transitions. It was quite clear that the transitions moved to a longer wavelength with the substitution of a proton with a carbon, and the greater the number of substitutions was, the greater the redshift in the UV spectrum was.

To explore whether the ENB unit had a UV absorbance in the range 200–250 nm, UV spectra of ethylidenecyclohexane and ENB units were calculated (Figure 2). Ethylidenecyclohexane

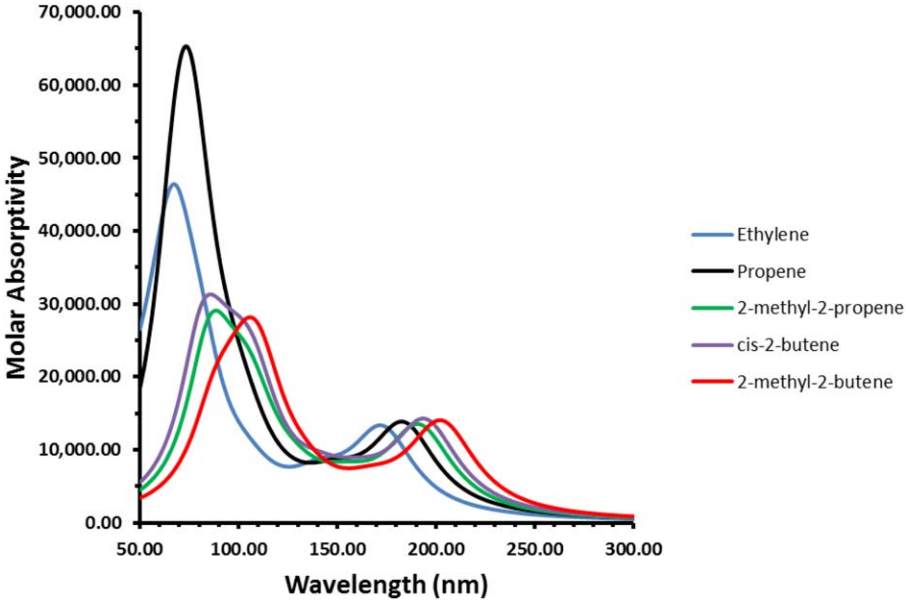

Figure 1. Gas-phase UV simulation of ethylene, propene, 2-methyl-2-propene, *cis*-2-butene, and 2-methyl-2-butene. [Color figure can be viewed in the online issue, which is available at wileyonlinelibrary.com.]

was chosen for the simulation because its double-bound structure was the same as that of ENB. It was also commercially available, and its calculated spectra could be verified with experiments. ENB (with a protonated double bond on the ring) was considered for the UV experiments. However, it was not commercially available, and it was difficult to synthesize to high purity. As shown in Figure 2, the ENB absorbance spectrum was similar to the one for ethylidenecyclohexane. There was a substantial UV absorptivity from 200 to 250 nm.

UV Spectroscopy of the Solvents and Model Compounds

As discussed previously in this article, the ENB structure might generate enough UV signal in the range 200–250 nm, but to observe it, we need to have solvents with a very low UV absorbance in this range. Therefore, the UV absorbances of some solvents were tested. $CDCl_3$ and $CHCl_3$ were chosen because a couple of EPDM elastomers with nearly equal ethylene and propylene contents could be dissolved in these two solvents at room temperature. The UV absorbances at 250 nm for $CDCl_3$ and $CHCl_3$ were 0.253 and 0.331 AU, respectively, with deionized (DI) water as a UV blank (Figure 3). For $CDCl_3$, the UV cutoff was 244 nm (UV absorbance = 1.021 AU at 243 nm). For $CHCl_3$, the UV cutoff was 245 nm (UV absorbance = 1.072 AU at 244 nm). These two solvents could be used for room-temperature SEC–UV analysis with a UV wavelength of slightly less than 250 nm and at 250 nm or greater. It is worth mentioning that a very small isotope effect was observed here.

TCE has a boiling point of 147 °C, is a good solvent for most of EPDM polymers, and could be a potential solvent for high-

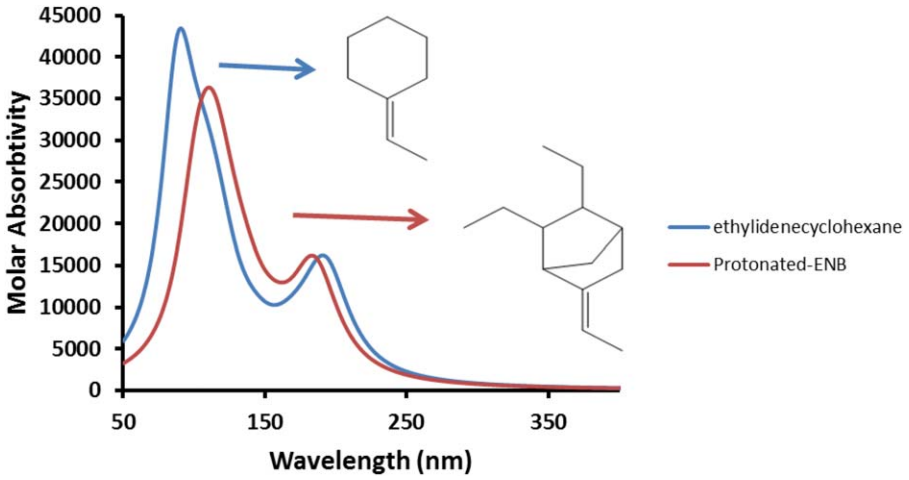

Figure 2. Gas-phase UV simulation of the ENB structure and ethylidenecyclohexane. [Color figure can be viewed in the online issue, which is available at wileyonlinelibrary.com.]

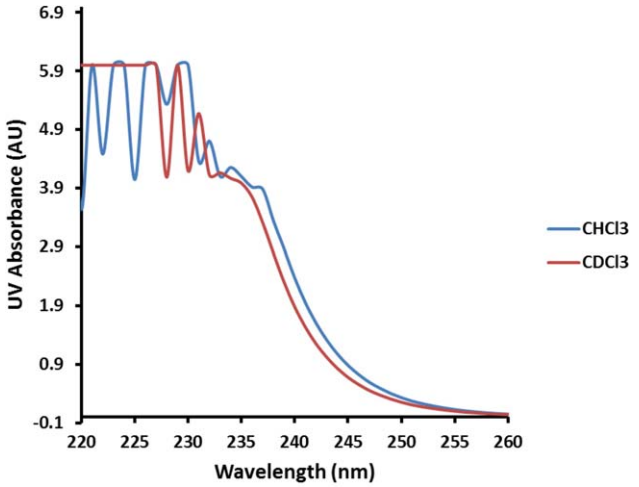

Figure 3. UV spectra of $CHCl_3$ and $CDCl_3$. DI water was used as the blank. [Color figure can be viewed in the online issue, which is available at wileyonlinelibrary.com.]

temperature SEC–UV. The UV spectra of TCE-d_2 and protonated TCEs are shown in Figure 4. TCE-d_2 was tested first, and the UV absorbance for TCE-d_2 at 250 nm was 0.210 AU. So, TCE-d_2 can be used for high-temperature SEC–UV experiments at 250 nm, although it was expensive. However, the protonated TCEs with the highest purity available from Sigma and Fluka had a significant UV absorbance at 250 nm. This strong UV absorbance at 250 nm was not expected to come from an isotope effect on the basis of the results shown in Figure 3. Impurities with UV chromophores were suspected in the protonated TCEs. GC/mass spectrometry (MS) was conducted, and the results are shown in the Supporting Information. Indeed, several chemicals that had a high UV absorbance at 250 nm were found. These two solvents could only be used in high-temperature SEC–UV around wavelengths of 250 nm and higher when the impurities responsible for the high UV absorbance at 250 nm were removed.

Decalin had a boiling point of 187 °C and was a good solvent for all of the EPDMs. Figure 5 shows the UV spectrum of decalin with DI water as a blank. The UV absorbance at 220 nm was 0.683 AU, and that at 230 nm was 0.292 AU. Decalin is a good potential solvent for high-temperature SEC–UV at slightly less than 220 nm and at 220 nm and greater.

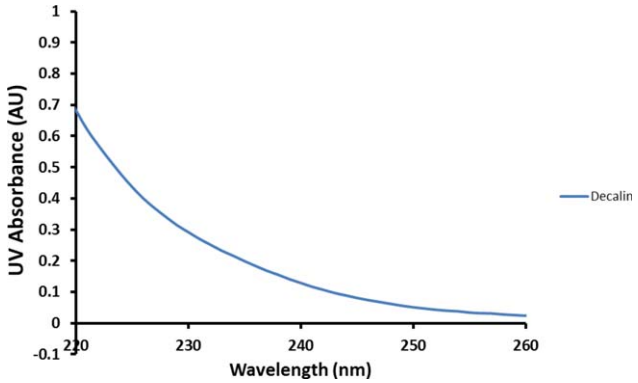

Figure 5. UV spectrum of decalin. DI water was used as the blank. [Color figure can be viewed in the online issue, which is available at wileyonlinelibrary.com.]

Decane and dodecane both have high boiling points (174 and 214 °C, respectively) and are potential solvents for high-temperature SEC–UV. However, as shown in Figure 6, decane had a strong UV absorbance at wavelengths of less than 242 nm (most likely because of impurities) and could only be used at wavelengths of 242 nm or greater. Dodecane had a much lower UV absorbance at 220 nm and higher wavelengths (Figure 6); this should be a good solvent for high-temperature SEC–UV at slightly less than 220 nm and at 220 nm and greater, although dodecane had some low-level UV chromophores, as shown by the GC–MS studies detailed in the Supporting Information. Decane could only be a potential high-temperature SEC–UV solvent if the impurities could be removed.

As mentioned previously, ethylidenecyclohexane had the same double-bond structure as ENB did in EPDM. Its UV absorbance was investigated experimentally, and the result is shown together with the potentially good high-temperature SEC–UV solvent

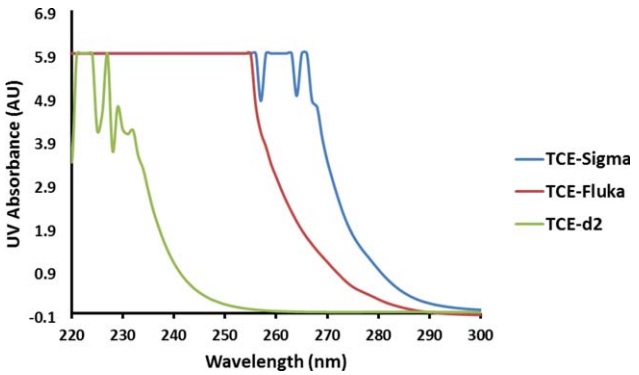

Figure 4. UV spectra of the TCE-d_2 and protonated TCEs. DI water was used as the blank. [Color figure can be viewed in the online issue, which is available at wileyonlinelibrary.com.]

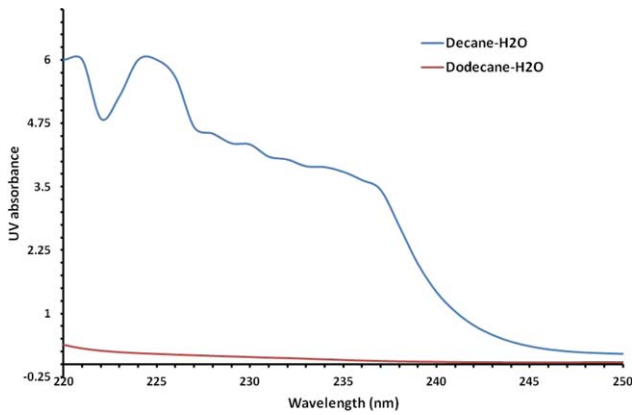

Figure 6. UV spectra of decane and dodecane. DI water was used as the blank. [Color figure can be viewed in the online issue, which is available at wileyonlinelibrary.com.]

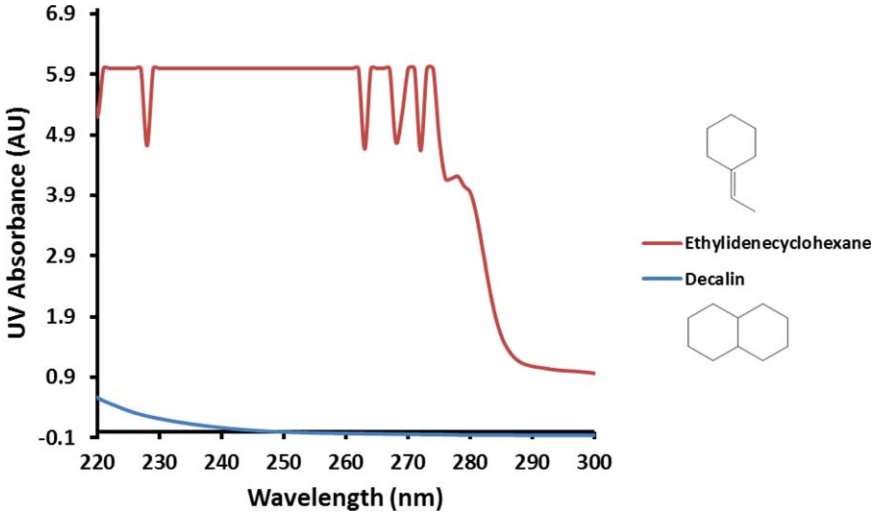

Figure 7. UV spectra of ethylidenecyclohexane and decalin. DI water was used as the blank. [Color figure can be viewed in the online issue, which is available at wileyonlinelibrary.com.]

decalin in Figure 7. In the range 220–280 nm, ethylidenecyclohexane had a strong UV absorbance. Although the trend was consistent with the gas-phase UV simulation shown in Figure 2, another possibility could be that there were some impurities that contributed to the strong UV absorbance. The low concentration of benzene (188 ppm), bromobenzene (121 ppm), and ketones (ca. 177 ppm) in ethylidenecyclohexane were detected (see the GC–MS and GC–flame ionization detector results in the Supporting Information). To understand the effects of these impurities, they were spiked into decalin at a slightly greater concentration then that measured by GC–MS: benzene (207 ppm), bromobenzene (128 ppm), and acetone (194 ppm; the sample preparation procedure was listed in the Supporting Information), and their UV spectra were compared with those of decalin and ethylidenecyclohexane (Figure 8). We observed that these impurities contributed little to the strong UV absorbance in the range 240–280 nm (bromobenzene did contribute some in the range 220–240 nm, but it did not account for all of the UV absorbed with ethylidenecyclohexane).

GC–UV of Ethylidenecyclohexane

Figure 9 shows the UV absorbance spectrum of ethylidenecyclohexane in the gas phase. We noted that this was an absorbance spectrum (i.e., concentration dependent), not an absorption cross section. The absorbance around 220 nm was clearly observed. On the basis of the results discussed previously, we observed the UV absorbance around 220 nm with the double-bond structure in ENB in EPDM. In the following sections, we explored the UV absorbance of the EPDM polymer samples.

UV/SEC–UV of the EPDM Polymers in $CDCl_3$ and $CHCl_3$

The UV absorbance of 1 wt % EPDM A and EPDM B in $CDCl_3$ was studied first (Figure 10). The blank used was $CDCl_3$. Because

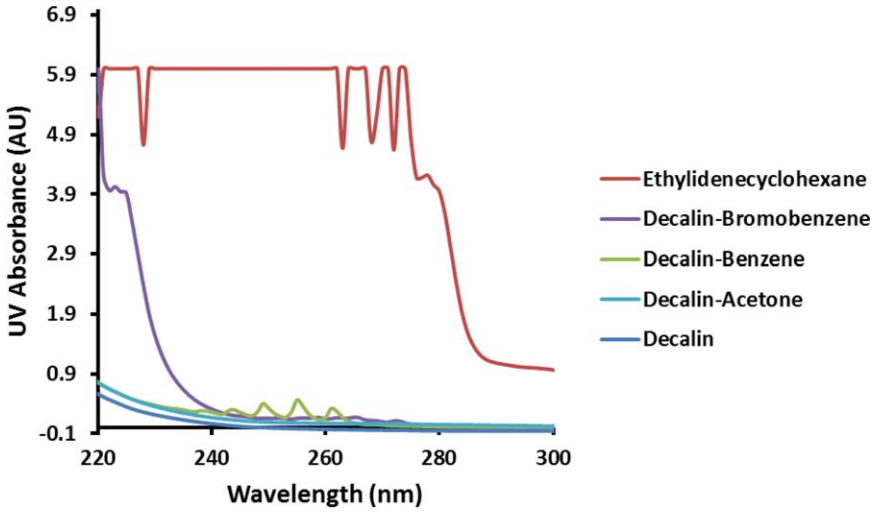

Figure 8. UV spectra of ethylidenecyclohexane, decalin, and decalin spiked with benzene, bromobenzene, and acetone. DI water was used as the blank. [Color figure can be viewed in the online issue, which is available at wileyonlinelibrary.com.]

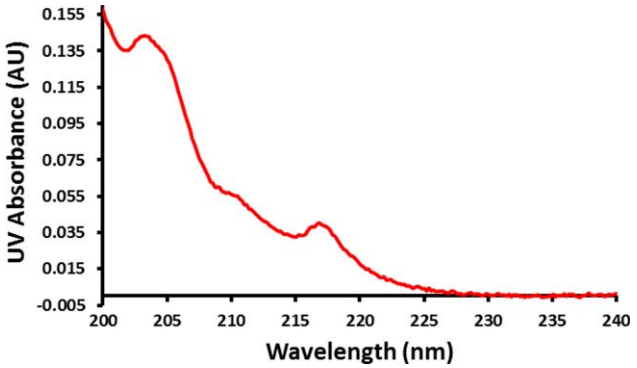

Figure 9. GC–UV spectrum of ethylidenecyclohexane. [Color figure can be viewed in the online issue, which is available at wileyonlinelibrary.com.]

of the strong UV absorbance of $CDCl_3$ itself at wavelengths of less than 240 nm, irregular peaks were observed at less than 240 nm. The UV absorbance at 250 nm for EPDM A and EPDM B were 0.589 and 0.372 AU, respectively. The ENB content in EPDM A was about five times that of the content in EPDM B (Table I). The discrepancy shown here at 250 nm could have been caused by different amounts of additives in the EPDMs.

To remove the effects of additives and other small molecules, SEC–UV–RI was explored. Figure 11 shows RI, UV at 250 nm and the ratio of UV/RI of the EPDM A. The UV intensity was multiplied by 40 times to match the RI signal. As UV signal was from the double bond in the ENB structure, the UV/RI ratio gave the ENB content along the MWD (elution time). We observed that for EPDM A, the ENB content was constant along with the molecular weight.

EPDM B was also studied with SEC–UV–RI. Figure 12 shows the RI, UV at 250 nm, and the UV/RI ratio of the EPDM B. The UV intensity was multiplied by 200 to match the RI. On the basis of the UV/RI ratio, the ENB content in EPDM B was also constant across the MWD. From the retention time shown in Figure 12, the molecular weight for EPDM B was higher than that of EPDM A.

Both EPDM A and EPDM B had an ENB content that did not vary with the molecular weight, although it was not surprising

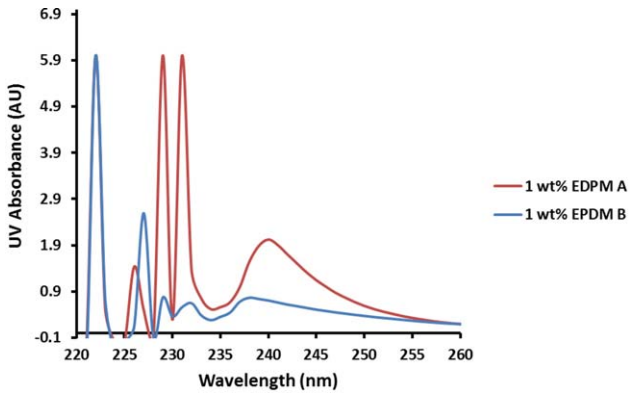

Figure 10. UV spectra of the polymers EPDM A and EPDM B in $CDCl_3$. $CDCl_3$ was used as the blank. [Color figure can be viewed in the online issue, which is available at wileyonlinelibrary.com.]

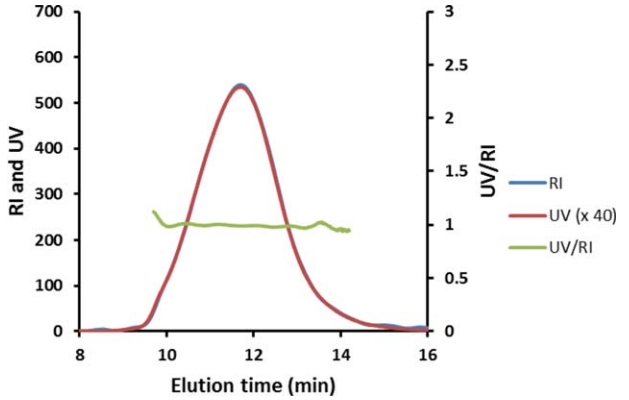

Figure 11. SEC–UV–RI of EPDM A at room temperature. The mobile phase was $CHCl_3$. The sample concentration was 10 mg/mL (injection = 100 µL, flow rate = 1 mL/min). The UV intensity was multiplied 40 times. [Color figure can be viewed in the online issue, which is available at wileyonlinelibrary.com.]

as they both were made with a single-site catalyst. To demonstrate the use of the UV/RI ratio for studying the ENB content in a heterogeneous system, a blend of EPDM A and EPDM B (1:1, w/w) was studied, and the results are shown in Figure 13. As discussed before, the EPDM B with a lower ENB content had a higher molecular weight, and the EPDM A with a higher ENB content had a lower molecular weight. The results in Figure 13 are consistent with expectations; that is, the ENB content increased as the molecular weight decreased. In other words, a blend of these two polymers was expected to produce an ENB content that varied across the MWD in the fashion observed in Figure 13. So far, the UV/RI ratio was used as an indication of the ENB content as a function of the molecular weight. To calculate the ENB content from the UV/RI ratio, the following method was developed.

Calibration of the UV and RI Detectors with EPDM Standards of Known Compositions

EPDM A and B were dissolved in $CHCl_3$ at a concentration of 10 mg/mL. The standard solution (100 µL) was injected into an

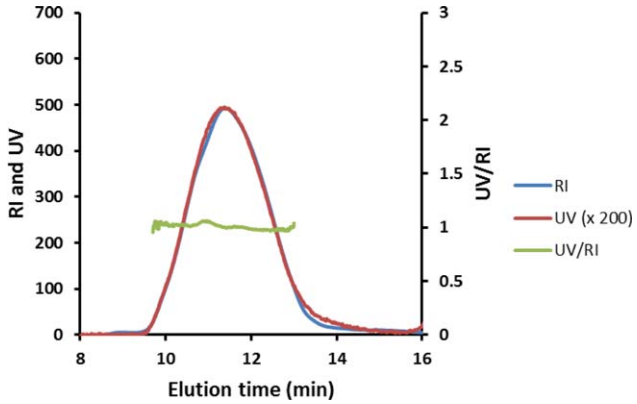

Figure 12. SEC–UV–RI of EPDM B at room temperature. The mobile phase was $CHCl_3$. The sample concentration was 10 mg/mL (injection = 100 µL, flow rate = 1 mL/min). The UV intensity was multiplied 200 times. [Color figure can be viewed in the online issue, which is available at wileyonlinelibrary.com.]

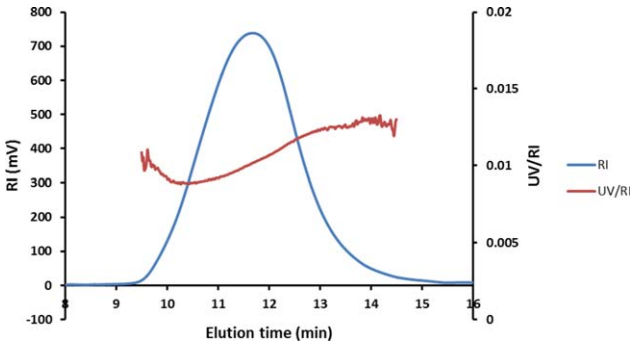

Figure 13. SEC–UV–RI of a 1:1 w/w blend of EPDM B and EPDM A at room temperature. The mobile phase was $CHCl_3$. The sample concentration was 10 mg/mL (injection = 100 μL, flow rate = 1 mL/min). [Color figure can be viewed in the online issue, which is available at wileyonlinelibrary.com.]

apparatus composed of a pump, an injector, an SEC column, a UV detector, and a RI detector. The RI and UV signals were collected as a function of time to generate the RI and UV chromatograms, respectively. The peak between 9 and 16 min in the RI chromatogram was integrated to generate a peak area [refractive-index peak area (A_{RI})]. The peak between 8 and 16 min in the UV chromatogram was integrated to generate the peak area [UV peak area (A_{UV})]. The integration was done with Cirrus software (version 3.1) from Agilent. The peak areas of two standards are listed in Table IV.

Each standard had a known composition predetermined by ^{13}C-NMR (Table I). Under a constant flow rate and constant data collection frequency, the total A_{UV} under the curve was equal to

$$A_{UV} = K_{UV,\,chromophore}\, m_{inj}\, W_{chromophore} \quad (1)$$

where m_{inj} is the injected mass of the polymer in the column (m_{inj} = Sample concentration × Injection volume), $K_{UV,\,chromophore}$ is the UV response factor of the comonomer with the chromophore in the polymer (see Table V), and $W_{chromophore}$ is the weight fraction of the comonomer with the chromophore in the polymer (here, the chromophore was from ENB in the polymerized form). Equation 1 can be rewritten as follows:

$$A_{UV,EPDM} = K_{UV,ENB}\, m_{inj}\, W_{ENB} \quad (2)$$

where $A_{UV,EPDM}$ is the UV peak area of the EPDM standard and W_{ENB} is the weight fraction of ENB in EPDM (Table I). Therefore, $K_{UV,ENB}$ can be determined from the UV peak area of the standard (see the results in Table V for $K_{UV,ENB}$; note that $K_{UVC2} = 0$ and $K_{UVC3} = 0$ and C_2 and C_3 represent the ethylene and propylene monomers, respectively):

$$K_{UV,ENB} = \frac{A_{UV,EPDM}}{m_{inj}\, W_{ENB}} \quad (3)$$

Table IV. A_{RI} and A_{UV} Values of the Two Standards from the SEC–UV–RI Experiment

	A_{RI} (mV s)	A_{UV} (mV s)
EPDM A	73,120	1850
EPDM B	63,940	340

Table V. K_{UV} and K_{RI} Values

$K_{UV,ENB}$ (mV s/mg)	$K_{RI,EP}$ (mV s/mg)	$K_{RI,ENB}$ (mV s/mg)
34,970	61,660	278,680

Under a constant flow rate and constant data-collection frequency

$$A_{RI} = m_{inj} \sum_i K_{RI,i}\, W_i \quad (4)$$

where m_{inj} is the injected mass of polymer into the column (m_{inj} = Sample concentration × Injection volume), $K_{RI,i}$ is the RI response factor of ith type monomer, and W_i is the weight fraction of ith type monomer in the polymer. For the case of EPDM, eq. 4 can be expanded to eq. 5 as follows:

$$A_{RI,EPDM} = K_{RI,C2}\, m_{inj}\, W_{C2} + K_{RI,C3}\, m_{inj}\, W_{C3} + K_{RI,ENB}\, m_{inj}\, W_{ENB} \quad (5)$$

where $A_{RI,EPDM}$ is the RI peak area of the EPDM standard; $K_{RI,C2}$, $K_{RI,C3}$, and $K_{RI,ENB}$ represent the RI response factors of ethylene, propylene, and ENB monomers, respectively; and W_{C2}, W_{C3} and W_{ENB} represent the weight fractions of ethylene, propylene and ENB monomer in EPDM, respectively. $K_{RI,i}$ is a product of a constant (K') and dn/dc of the homopolymer of monomer i (dn/dc_i) as follows:

$$K_{RI,i} = K'\, dn/dc_i \quad (6)$$

where K' is a constant for the same RI detector and the same experimental conditions. The dn/dc of polyethylene and the dn/dc of polypropylene had the same value.[26] Therefore, $K_{RI,C2} = K_{RI,C3}$. Note, the dn/dc value for a particular monomer (polymerized) could also be measured with the standard homopolymer of that monomer, and an RI detector at the same eluent and temperature (T_1) as that used for the unknown polymer sample of interest. The first two terms on the right side of eq. 5 could be combined, as follows:

$$A_{RI,EPDM} = K_{RI,EP}\, m_{inj}(1 - W_{ENB}) + K_{RI,ENB}\, m_{inj}\, W_{ENB} \quad (7)$$

where $K_{RI,EP}$ is the RI response factor of either ethylene or propylene monomer. The weight fractions of the ethylene and propylene monomers in EPDM were equal to $1 - W_{ENB}$. For the two standards EPDM A and EPDM B, two equations were obtained from eq. 7 as follows:

$$A_{RI,EPDM\,A} = K_{RI,EP}\, m_{inj,EPDM\,A}(1 - W_{ENB,EPDM\,A}) + K_{RI,ENB}\, m_{inj,EPDM\,A}\, W_{ENB,EPDM\,A} \quad (8)$$

$$A_{RI,EPDM\,B} = K_{RI,EP}\, m_{inj,EPDM\,B}(1 - W_{ENB,EPDM\,B}) + K_{RI,ENB}\, m_{inj,EPDM\,B}\, W_{ENB,EPDM\,B} \quad (9)$$

Equation 8 can be rearranged to move $K_{RI,EP}$ to the left side of the equation with $A_{RI,EPDM\ A}$, the injected mass of EPDM A ($m_{inj,EPDM\ A}$), and ENB content of EPDM A ($W_{ENB,EPDM\ A}$), as follows:

$$K_{RI,EP} = \frac{A_{RI,EPDM\,A} - K_{RI,ENB}\, m_{inj,EPDM\,A}\, W_{ENB,EPDM\,A}}{m_{inj,EPDM\,A}(1 - W_{ENB,EPDM\,A})} \quad (10)$$

$K_{RI,EP}$ of eq. 10 was plugged into eq. 9 with $A_{RI,\ EPDM\ B}$, the injected mass of EPDM B ($m_{inj,EPDM\ B}$), and the ENB content of EPDM B ($W_{ENB,EPDM\ B}$), as follows:

$$A_{RI,EPDM\ B} = S * (A_{RI,EPDM\,A} - K_{RI,ENB}\, m_{inj,EPDM\,A}\, W_{ENB,EPDM\,A}) + K_{RI,ENB}\, m_{inj,EPDM\,B}\, W_{ENB,EPDM\,B} \quad (11)$$

where S is as follows:

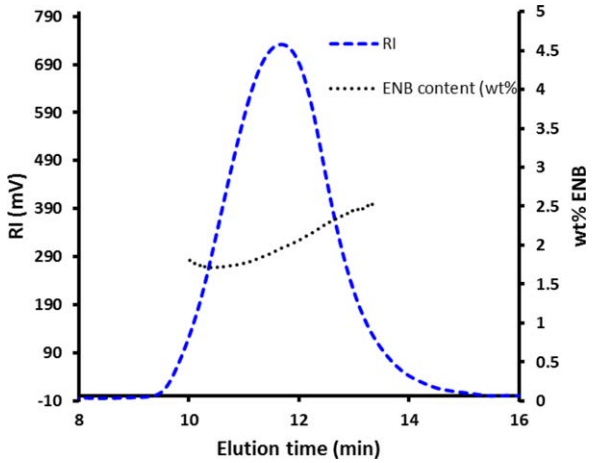

Figure 14. ENB content of a 1:1 w/w blend of EPDM B and EPDM A at room temperature. The mobile phase was $CHCl_3$. The sample concentration was 10 mg/mL (injection = 100 μL, flow rate = 1 mL/min). [Color figure can be viewed in the online issue, which is available at wileyonlinelibrary.com.]

$$S = \frac{m_{\text{inj,EPDM B}}(1 - W_{\text{ENB,EPDM B}})}{m_{\text{inj,EPDM A}}(1 - W_{\text{ENB,EPDM A}})} \tag{12}$$

Equation 11 is rearranged to move $K_{\text{RI,ENB}}$ at the left side of equation, as follows:

$$K_{\text{RI,ENB}} = \frac{A_{\text{RI, EPDM B}} - SA_{\text{RI,EPDM A}}}{m_{\text{inj,EPDM B}} W_{\text{ENB,EPDM B}} - Sm_{\text{inj,EPDM A}} W_{\text{ENB,EPDM A}}} \tag{13}$$

Therefore, $K_{\text{RI,ENB}}$ is determined from the injected mass, the A_{RI} values, and the W_{ENB} values of the two standards. When $K_{\text{RI,ENB}}$ is known, $K_{\text{RI,EP}}$ can be determined from eq. 10. After this calibration step, the K_{UV} and K_{RI} values, $K_{\text{UV,ENB}}$, $K_{\text{RI,EP}}$, and $K_{\text{RI,ENB}}$, were determined and are listed in Table V, shown later.

Measurement of the ENB Content at Each Elution Time

The ENB content at each elution time i ($W_{\text{ENB},i}$) was determined from the UV signal at elution time i and the RI signal at elution time $i + \Delta i$, where Δi is the time interval between the UV and RI detectors. Δi was calculated from the difference in the peak retention time of a polystyrene standard with a polydispersity of less than 1.1 (peak molecular weight ≈ 200,000 g/mol). The polystyrene standard was run with the same conditions as those used in the previous calibration. After the adjustment of the time interval, the UV/RI ratio at each elution time was calculated. See Figure 11 for an example with the UV/RI ratio overlaid on the RI and UV chromatogram. From eqs. 2 and 7, the following equation can be derived through the replacement of A_{UV} and A_{RI} with UV and RI signals at elution time i as follows:

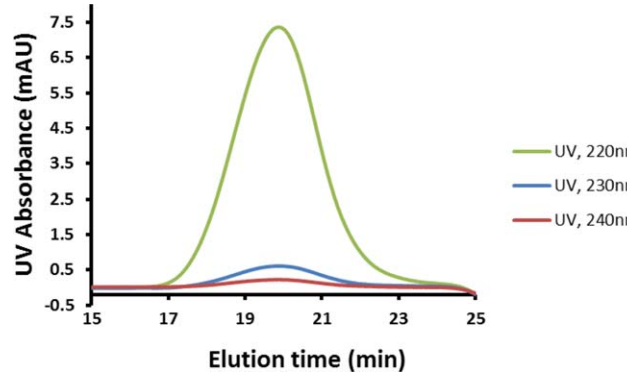

Figure 15. SEC–UV of EPDM A in decalin at 45 °C. The sample concentration was 2.7 mg/mL (injection = 100 μL). [Color figure can be viewed in the online issue, which is available at wileyonlinelibrary.com.]

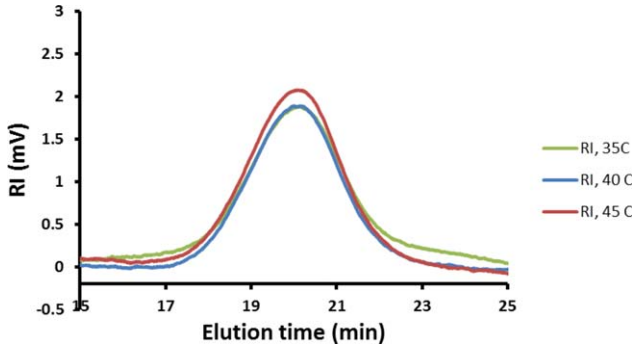

Figure 16. RI of EPDM A in decalin at different temperatures. The sample concentration was 2.7 mg/mL (injection = 100 μL). [Color figure can be viewed in the online issue, which is available at wileyonlinelibrary.com.]

$$\frac{\text{UV}_i}{\text{RI}_{i+\Delta i}} = \frac{K_{\text{UV,ENB}} m_{\text{inj}} w_{\text{EPDM},i} W_{\text{ENB},i}}{K_{\text{RI,EP}} m_{\text{inj}} w_{\text{EPDM},i}(1 - W_{\text{ENB},i}) + K_{\text{RI,ENB}} m_{\text{inj}} w_{\text{EPDM},i} W_{\text{ENB},i}} \tag{14}$$

where $w_{\text{EPDM},i}$ is the weight fraction of the polymer at elution time i. The weight fraction and m_{inj} terms can be cancelled because each is present in both the numerator and the denominator as follows:

$$\frac{\text{UV}_i}{\text{RI}_{i+\Delta i}} = \frac{K_{\text{UV,ENB}} W_{\text{ENB},i}}{K_{\text{RI,EP}}(1 - W_{\text{ENB},i}) + K_{\text{RI,ENB}} W_{\text{ENB},i}} \tag{15}$$

Equation 15 is rearranged to move $W_{\text{ENB},i}$ to the left side of the equation as follows:

$$W_{\text{ENB},i} = \frac{\frac{\text{UV}_i}{\text{RI}_{i+\Delta i}} K_{\text{RI,EP}}}{K_{\text{UV,ENB}} + \frac{\text{UV}_i}{\text{RI}_{i+\Delta i}} K_{\text{RI,EP}} - \frac{\text{UV}_i}{\text{RI}_{i+\Delta i}} K_{\text{RI,ENB}}} \tag{16}$$

With the K_{UV} and K_{RI} values obtained in the calibration step, $W_{\text{ENB},i}$ is calculated at each elution time with eq. 16. The ENB content by weight percentage is converted from a weight fraction by the following equation:

$$\text{wt \% ENB}_i = W_{\text{ENB},i} \times 100 \tag{17}$$

The ENB content across the MWD for the 1:1 w/w blend of EPDM A and EPDM B previously shown in Figure 13 is quantitatively described in Figure 14.

SEC–UV–RI of EPDM A in Decalin

It is clear from the previous discussion that ENB in EPDM had enough UV absorbance at 250 nm in $CHCl_3$ to study the ENB content across the MWD. However, most commercial EPDM products are not soluble at low temperatures, so the use of decalin, a high-boiling-point solvent, as the eluent was explored. We were initially surprised when we found that no UV absorbance at 250 nm was observed for EPDM A in decalin, even on

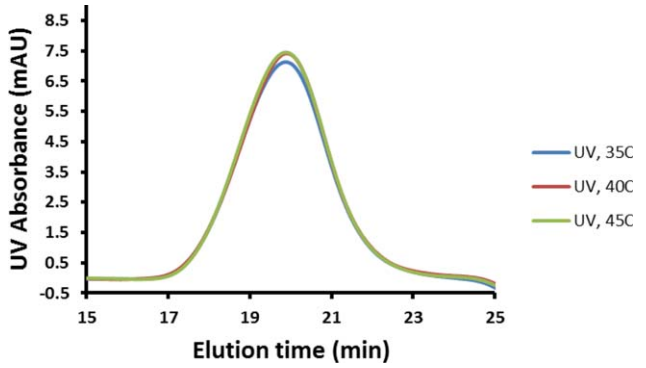

Figure 17. SEC–UV–RI at 220 nm of EPDM A in decalin at different temperatures. The sample concentration was 2.7 mg/mL (injection = 100 μL). [Color figure can be viewed in the online issue, which is available at wileyonlinelibrary.com.]

different instruments. We found this to be related to the solvent polarity.[27] The polarity of $CHCl_3$ relative to that of water was about 0.26, but the polarity of decalin relative to that of water was almost zero. In alkenes, among the available σ–σ* and π–π* transitions, the π–π* transitions are of the lowest energy. The transition energy depends on the solvent polarity. For example, in case of π–π* transitions, the excited states are more polar than the ground state, and the dipole–dipole interactions with solvent molecules lower the energy of the excited state more than that of the ground state. Therefore, a polar solvent decreases the energy of π–π* transitions and the absorbance maximum appears redshifted. This means that the UV absorbance wavelength of ENB in decalin could be lower than 250 nm; this was the wavelength used for SEC–UV–RI with $CHCl_3$. SEC–UV of EPDM A in decalin at 220, 230, and 240 nm at 45 °C was then explored, and the results are shown in Figure 15. A strong UV absorbance was observed at 220 nm, and the UV absorbance was weaker at 230 and 240 nm. Because the boiling point of decalin was 187 °C, it was possible to study the ENB content in all of the EPDMs along the MWD with high-temperature SEC–UV–RI with decalin as the eluent. Other solvents, such as dodecane, as discussed earlier, were also possible. As for TCE and decane, impurities with a strong UV absorbance needed to be removed before the material was used as an eluent. Long alkyl chain alcohols, such as 2-octanol, might also be potential solvent candidates, and alcohol might give a UV absorbance redshift because of its polarity.

For high-temperature SEC–UV–RI with decalin and the other potential solvents discussed previously, one may be concerned with the specific dn/dc of a solution, which is defined as follows:

$$dn/dc = (n - n_1)/c$$

where n, n_1, and c are the indices of refraction for the solution and solvent and the concentration of solute (g/mL), respectively. Chiang[28] studied the temperature dependence of the specific dn/dc values of polyethylene in various solvents, and reported that dn/dc increased with increasing temperature [$d(dn/dc)dt = 2.43 \times 10^{-4}$], and dn/dc was 0.0917 at 80 °C in *n*-decane. To explore this temperature effect, the RI of EPDM A in decalin at different temperatures was studied (Figure 16). The RI areas were 294, 309, and 316 mV s at 35, 40, and 45 °C, respectively. So, the dn/dc of the polymer with decalin at high temperature was significant enough to monitor EPDM with a differential refractometer on SEC–UV–RI.

Another concern of the high-temperature SEC–UV–RI of EPDM is the effect of the temperature on the UV absorbance. Strong UV absorbance was observed at room temperature (Figure 15), and it is desirable to have a positive effect of the temperature on the UV absorbance. That is, the UV absorbance is stronger at higher temperatures. Fahr and Nayak[29] studied the temperature dependence of the UV absorbance of 1,3-butadiene in the gas phase and found that the UV absorbance in the range 220–240 nm increased with increasing temperature. A similar phenomenon was observed with propylene.[30] SEC–UV of EPDM A at 35, 40, and 45 °C was explored, and the results are shown in Figure 17. The A_{UV} values at 35, 40 and 45 °C were 1149, 1171, and 1196 mAU s, respectively. The UV absorbance appeared to increase with increasing temperature, so the detection of UV of ENB at high temperature is not expected to have issues.

CONCLUSIONS

In this article, we revealed that the double bond in ENB had a reasonable UV absorbance at 220–250 nm with UV simulation. We found that solvents, such as decalin and dodecane, had a low UV absorbance in this UV range. These solvents had high boiling points, and these are essential for high-temperature SEC–UV–RI. We proved the UV absorbance of the ENB double-bond structure with a model compound that had the same double-bond structure and demonstrated the feasibility of obtaining ENB content as a function of the molecular weight of EPDM with SEC–UV–RI. These findings should enable the simultaneous determination of the EPDM MWD and ENB content as a function of the molecular weight for a wide range of EPDM polymers when applied with a high-temperature SEC–UV–RI. This UV absorption-based detection concept could also be used for other polymers that contain a UV chromophore and require high temperatures for dissolution, including the quantification of additives with a UV chromophore in polymers. This includes polymers containing vinyl, conjugated vinyl, aromatic, carbonyl, or halocarbon groups. This concept may also be extended to high-temperature thermal-gradient interactive chromatography-UV, high-temperature solvent-gradient interactive chromatography-UV (high-temperature liquid chromatography-UV), temperature-rising elution fractionation-UV, crystallization analysis fractionation-UV, crystallization elution fractionation-UV, and other high-temperature hyphenated techniques-UV.

ACKNOWLEDGMENTS

The authors thank Steve Erskine, Dave Schiff, and David Meunier for providing helpful information and for their discussions.

REFERENCES

1. (a) Borg, E. L. In Rubber Technology, 2nd ed.; Morton, M., Ed.; Krieger: Malabar, FL, **1981**; (b) Hofmann, W. In Rubber Technology Handbook; Hanser: Munich, **1989**.
2. Allen, R. D. J. *Elastomers Plast.* **1983**, *15*, 19.
3. Chitta, R.; Ginzburg, A.; van Doremaele, G.; Macko, T.; Brüll, R. *Polymer* **2011**, *52*, 5953.
4. Striegel, A.; Yau, W. W.; Kirkland, J. J.; Bly, D. D. In Modern Size Exclusion Liquid Chromatography; Wiley: New York, **2009**.
5. Ute, K.; Niimi, R.; Hatada, K.; Kolbert, A. C. *Int. J. Polym. Anal. Char.* **1999**, *5*, 47.
6. Hatada, K.; Ute, K.; Kitayama, T.; Yamamoto, M.; Nishimura, T.; Kashiyama, M. *Polym. Bull.* **1989**, *21*, 489.
7. Hatada, K.; Ute, K.; Kitayama, T.; Nishimura, T.; Kashiyama, M.; Fujimoto, N. *Polym. Bull.* **1990**, *22*, 549.
8. Ute, K.; Niimi, R.; Hongo, S.; Hatada, K. *Polym. J.* **1998**, *30*, 439.
9. Loucks, D. A. U.S. Pat. 4,983,528 (**1991**).
10. Qian, X. Y.; Nagashima, K. *Kogakuin Daigaku Kenkyu Hokoku* **1993**, *75*, 139.
11. Mayeda, S.; Nagata, M. *J. Appl. Polym. Sci. Appl. Polym. Symp.* **1993**, *52*, 173.
12. Anderson, J. N. *J. Appl. Polym. Sci.* **1974**, *18*, 2819.
13. Tackx, P.; Bremmers, S. *Polym. Mater. Sci. Eng.* **1998**, *78*, 50.
14. Hiller, W.; Pasch, H.; Macko, T.; Hofmann, M.; Ganz, J.; Spraul, M.; Braumann, U.; Streck, R.; Mason, J.; Van Damme, F. *J. Magn. Reson.* **2006**,*183*, 290.
15. Housaki, T. *Polym. J.* **1988**, *20*, 1163.
16. Cong, R.; deGroot, A. W.; Parrott, A.; Yau, W.; Hazlitt, L.; Brown, R.; Miller, M. D.; Zhou, Z. *Macromolecules* **2011**, *44*, 3062.
17. Miller, M. D; deGroot, A. W.; Lyons, J.; Van Damme, F.; Winniford, B. *J. Appl. Polym. Sci.* **2011**, *123*, 1238.
18. Winniford, B.; Cong, R.; Stokich, T. M.; Pell, R. J.; Miller, M. D.; Roy, A.; van Damme, F.; deGroot, A. W.; Lyons, J. W.; Meunier, D. M. U.S. Pat. 8,318,896 (**2012**).
19. Wild, L. *Adv. Polym. Sci.* **1991**, *98*, 1.
20. Monrabal, B. *J. Appl. Polym. Sci.* **1994**, *52*, 491.
21. Monrabal, B. J.; Sancho-Tello, J.; Mayo, N.; Romero, L. *Macromol. Symp.* **2007**, *257*, 71.
22. Frisch, M. J.; Trucks, G. W.; Schlegel, H. B. In Gaussian 09, Revision A.02; Gaussian: Wallingford, CT, **2004**.
23. (a) Becke, A. D. *J. Chem. Phys.* **1993**, *98*, 5648; (b) Hohenberg, P.; Kohn, W. *Phys. Rev. B* **1964**, *136*, 864; (c) Becke, A. D. *Phys. Rev. A* **1988**, *38*, 3098; (d) Vosko, S. H.; Wilk, L.; Nusair, M. *Can. J. Phys.* **1980**, *58*, 1200; (e) Lee, C.; Yang, W.; Parr, R. G. *Phys. Rev. B* **1988**, *37*, 785; (f) Miehlich, B.; Savin, A.; Stoll, H.; Preuss, H. *Chem. Phys. Lett.* **1989**, *157*, 200.
24. (a) Ridley, J.; Zerner, M. *Theor. Chim. Acta* **1973**, *32*, 111; (b) Ridley, J. E.; Zerner, M. C. *Theor. Chim. Acta* **1976**, *42*, 223; (c) Bacon, A. D.; Zerner, M. C. *Theor. Chim. Acta* **1979**, *53*, 21; (d) Anderson, W. P.; Edwards, W. D.; Zerner, M. C. *Inorg. Chem.* **1986**, *25*, 2728; (e) Zerner, M. C.; Lowe, G. H.; Kirchner, R. F.; Mueller-Westerhoff, U. T. *J. Am. Chem. Soc.* **1980**,*102*, 589; (f) Thompson, M. A.; Zerner, M. C. *J. Am. Chem. Soc.* **1991**,*113*, 8210; (g) Zerner, M. C.; Correa de Mello, P.; Hehenberger, M. *Int. J. Quant. Chem.* **1982**, *21*, 251; (h) Hanson, L. K.; Fajer, J.; Thompson, M. A.; Zerner, M. C. *J. Am. Chem. Soc.* **1987**, *109*, 4728; (i) Zerner, M. C. In Review of Computational Chemistry; Lipkowitz, K. B., Boyd, D. B., Eds.; VCH: New York, **1991**; Vol. *2*, p 313.
25. Schug, K. A.; Sawicki, I.; Carlton, D. D.; Fan, H.; McNair, H. M.; Nimmo, J. P.; Kroll, P.; Smuts, J.; Walsh, P.; Harrison, D. *Anal. Chem.* **2014**, *86*, 8329.
26. Brandrup, J., Ed. In Polymer Handbook, 4th ed.; Wiley-Interscience: New York, **1999**.
27. Agilent Technologies. In Fundamentals of UV–Visible Spectroscopy (Workbook); Agilent Technologies: Waldbronn, Germany, **2000**; p 21.
28. Chiang, R. *J. Polym. Sci. Part C: Polym. Symp.* **1965**, *8*, 295.
29. Fahr, A.; Nayak, A. K. *Chem. Phys.* **1994**, *189*, 725.
30. Fahr, A.; Nayak, A. K. *Chem. Phys.* **1996**, *203*, 351.